

# CdS-sensitized solar cell based on screen-printed TiO<sub>2</sub> nanoporous electrode

XIAOTAO SUI, TAO ZENG, GUANCHAO YIN, HAO CHENG, XIUJIAN ZHAO\*

*Key Laboratory of Silicate Materials Science and Engineering (Wuhan University of Technology), Ministry of Education, 122 Luoshi-Road, Hongshan District, Wuhan 430070, Hubei, People's Republic of China*

CdS quantum dots sensitized solar cells (QDSCs) based on screen-printed TiO<sub>2</sub> nanoporous electrodes were assembled. The TiO<sub>2</sub> nanoporous films were prepared by screen-printing technique which the thickness of TiO<sub>2</sub> film was controlled through the screen printing cycles. The CdS quantum dots (QDs) were grown by the successive ionic layer adsorption and reaction deposition method. The efficiencies of the CdS-sensitized TiO<sub>2</sub> solar cells were increased with the increasing the screen printing cycles. The assembled CdS QDSCs yield a best power conversion efficiency of 1.34% and a short-circuit current of 3.1 mA/cm<sup>2</sup> with carbon counter electrode.

(Received February 28, 2011; accepted March 16, 2011)

*Keywords:* Sensitized solar cell, Screen printing, Successive ionic layer adsorption and reaction, Quantum dots

## 1. Introduction

Quantum dots sensitized solar cells (QDSCs) have attracted great attention in the area of solar energy applications. In general, QDSCs consist of porous TiO<sub>2</sub> photoanode sensitized by semiconductor quantum dots (QDs) and platinum cathode with polysulfide (S<sup>2-</sup>/Sx<sup>2-</sup>) electrolyte [1]. In QDSCs, metal chalcogenide QDs (such as CdS [2, 3], CdSe [4, 5], PbS [6], Ag<sub>2</sub>S [7], Bi<sub>2</sub>S<sub>3</sub> [8] and CdTe [9]) are usually served as sensitizers because they can absorb light in the visible region. Compared with conventional dyes, the advantages of a QD sensitizer include higher extinction coefficients [10], large intrinsic dipole moment [11] and multiple exciton generation by impact ionization [12]. The most commonly used QD sensitizer was cadmium sulfide (CdS), which it has large optical absorption in the visible range and appropriate band alignment between CdS and TiO<sub>2</sub>. Moreover, quantum effects in CdS QDs have been widely studied and methods of controlling the size of CdS QDs are well-established. Therefore, much of the work related to QDSCs has been performed on CdS QDSCs [13-15].

Titanium dioxide (TiO<sub>2</sub>) is the best choice in semiconductor oxides in QDSCs till now due to low-cost price, abundance in the market, nontoxicity, and biocompatibility. The two main selected deposition processes widely used to prepare TiO<sub>2</sub> films are doctor-blading and screen-printing technique. Screen-printing of TiO<sub>2</sub> is a widespread industrially-applied method because its fast-printing technique, controllable thickness and uniform morphologies.

In QDSCs, Pt is generally used as counter electrode because Pt exhibits excellent catalytic activity and good electric conductivity. However, Pt is rare metal and extremely expensive [16]. Thus, it is necessary for counter

electrode to develop lower cost materials which has high electrochemical activity. So far, inexpensive carbonaceous materials such as graphite, carbon black, activated carbon, hard carbon sphere, carbon nanotube, fullerene and graphene, have been employed as the catalysts for counter electrodes [17-24].

In this work we report on CdS QDs sensitized TiO<sub>2</sub> solar cells, in which TiO<sub>2</sub> films were prepared using screen printing technique and CdS QDs were synthesized by successive ionic layer adsorption and reaction deposition (SILAR). We investigated the dependence of the photovoltaic parameters on the screen printing cycles and the counter electrodes. The as-synthesized cell shows a maximum conversion efficiency of 1.34% with carbon counter electrode under one sun illumination when the TiO<sub>2</sub> film was prepared through six screen printing cycles.

## 2 Experimental

### 2.1 Screen-printing synthesis of TiO<sub>2</sub> nanoporous electrode

Nanoporous TiO<sub>2</sub> films were prepared by spreading a commercial TiO<sub>2</sub> paste (DHS-TPP2) onto fluorine-doped tin oxide (FTO) glass (15Ω/□) using the screen printing method, followed by sintering at 500 °C for 3 hours. A thicker TiO<sub>2</sub> layer can be obtained by repeating the screen printing operation. Samples went through screen printing cycles *n*, herein referred to as TiO<sub>2</sub>(*n*) (*n* = 3,4,5,6).

### 2.2 Preparation of CdS sensitized TiO<sub>2</sub> electrode

CdS QDs were synthesized using SILAR method [13]. A TiO<sub>2</sub> film was dipped into a 0.5 M Cd(NO<sub>3</sub>)<sub>2</sub> aqueous

solution for 5 min, rinsed with deionized water, and then dipped for another 5 min into a 0.5 M Na<sub>2</sub>S aqueous solution and rinsed again with deionized water. The two-step dipping procedure forms one SILAR cycle. Samples went through 5 SILAR cycles in our experiments.

The CdS-sensitized TiO<sub>2</sub> electrode and the counter-electrode were sandwiched using a 60 μm-thick parafilm spacer. The Pt counter electrode was prepared by dripping a drop of 5 mM H<sub>2</sub>PtCl<sub>6</sub> ethanol solution onto a FTO glass substrate, followed by heating at 400 °C for 15 min. A carbon electrode on FTO was prepared according to a previous work [17]. The liquid electrolyte consisted of 0.5 M 1-butyl-3-methylimidazolium iodide, 0.05 M I<sub>2</sub>, 0.5 M 4-tert-butylpyridine and 0.1 M guanidine thiocyanate in acetonitrile.

### 2.3 Characterization

The absorption spectra were recorded with a Hitachi UV-vis 3600A spectrophotometer. Field emission scanning electron microscopy (FESEM) images were made with a Hitachi FE-4800. Energy dispersive spectroscopy (EDS) measurements were made with JSM-5610LV. The photocurrent-voltage (I-V) curve was measured under an illumination of a solar simulator (Newport, Oriel class B) at one sun (AM1.5, 100 mW cm<sup>-2</sup>). An Eco Chemie Autolab potentiostat/galvanostat was used to record the current-voltage (I-V) characteristics. The active area of the cell was 0.23 cm<sup>2</sup>.

### 3. Results and discussion

The surface morphology of TiO<sub>2</sub> nanoporous films before and after CdS deposition were examined by FESEM and the images are shown in Fig. 1a and b. As can be seen in Fig. 1a, the TiO<sub>2</sub> film prepared by screen printing technique shows highly porous network and the particle size of TiO<sub>2</sub> nanoparticles ranges from 25-50 nm. Fig. 1b shows that the surface morphology of TiO<sub>2</sub>/CdS film. Compared with Fig. 1a, it can be easily determined that CdS QDs have been deposited on the TiO<sub>2</sub> nanoporous film and the particle size of CdS QDs was about 10 nm. Besides, larger pores can also be observed in the TiO<sub>2</sub> nanoporous film which would facilitate the penetration of CdS depositions solutions to TiO<sub>2</sub> nanoporous film. The sample composition was identified by EDS analysis (Fig. 1c and d) performed inside the FESEM. Fig. 1c shows that Ti and O peaks are derived from the TiO<sub>2</sub> film prepared by screen printing method. Besides Ti and O peaks from TiO<sub>2</sub> nanoparticles, Cd and S peaks in the EDS spectrum reveal that the QDs deposited inside TiO<sub>2</sub> films are mainly composed of cadmium and sulfur. Quantitative analysis of the EDS spectrum gives a Cd/S atomic ratio of about 1:1, indicating that high-grade CdS QDs were formed inside the TiO<sub>2</sub> films.

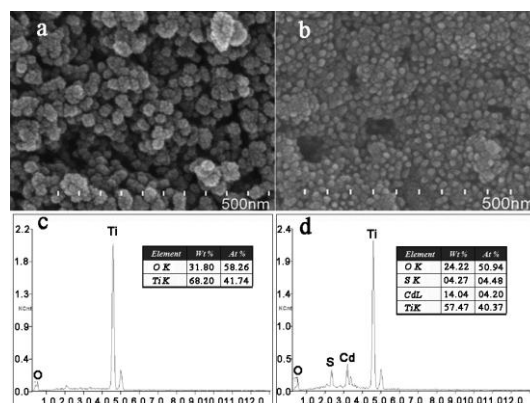


Fig.1. FESEM images of TiO<sub>2</sub> nanoporous films before (a) and after (b) CdS deposition. EDS spectra of the plain TiO<sub>2</sub> film (c) and CdS/TiO<sub>2</sub> film (d).

Fig. 2 shows the UV-vis absorption spectra of the plain TiO<sub>2</sub> film and the TiO<sub>2</sub>(n)/CdS films (n=3,4,5,6) between 300 and 600 nm in wavelength. Compared with the absorption spectrum of plain TiO<sub>2</sub> film, there is an obvious absorption peak near 550 nm for CdS sensitized TiO<sub>2</sub> films, which is ascribed to the contribution from CdS QDs. In addition, the thickness of the screen-printed TiO<sub>2</sub> nanoporous film was controlled by the cycles of screen printing operation. The thickness of the screen-printed TiO<sub>2</sub> nanoporous film was about 2 μm through one screen printing cycle. The cycles of screen printing were from 3 to 6. It is clearly found that the absorbance of CdS sensitized electrode is increased with the increasing screen printing cycles, indicating that more CdS QDs have been deposited on the thicker TiO<sub>2</sub> film at the same SILAR cycles of QDs. Such an increase of CdS amount should be due to the increase of specific surface area when the thickness of TiO<sub>2</sub> film is increased.

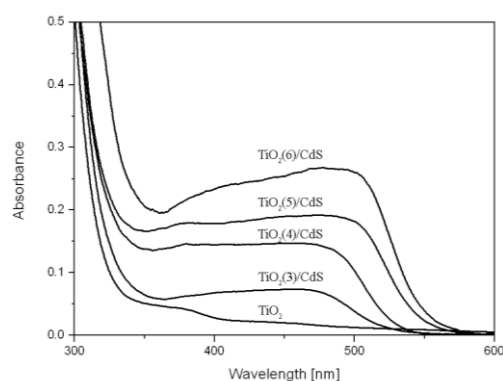


Fig. 2. UV-vis absorption spectra of CdS QDs sensitized TiO<sub>2</sub> films with different screen printing cycles.

The photocurrent-voltage (J-V) characteristics of TiO<sub>2</sub>(n)/CdS electrodes with Pt and carbon counter electrode under AM1.5 illumination are shown in Fig. 3. When illuminated, CdS QDs can effectively absorb visible lights (with absorption edge at ~550 nm) and thus excite electrons from the valence band (VB) to the conduction band (CB) in the QDs while holes left behind in the VB.

Because the CB of CdS QDs is above that of the TiO<sub>2</sub> nanoparticle [25], local band bending occurs at the TiO<sub>2</sub>/CdS interface, which results in a local electric field injecting the photogenerated electrons into the CB of TiO<sub>2</sub>. Since the TiO<sub>2</sub> nanoparticles are crystalline, the injected electrons can be transferred effectively to the collector electrode. Thus, the CdS QDs sensitized TiO<sub>2</sub> nanoporous electrodes have an ability of transferring light energy to electric energy under illumination. The difference on the photovoltaic performance with the increasing the screen printing cycles can be observed. As shown in Fig. 3a, when used Pt counter electrode, both short-circuit photocurrent density ( $J_{sc}$ ) and power conversion efficiency ( $\eta$ ) increased quickly from 0.8 mA cm<sup>-2</sup>, 0.27% to 2.2 mA cm<sup>-2</sup>, 0.91%. It is due to that with the screen printing cycles increased, the thickness of TiO<sub>2</sub> nanoporous film and the amount of the CdS QDs will be increased, thus giving higher  $J_{sc}$  and conversion efficiency ( $\eta$ ) of QDSCs. A similar observation was made in the TiO<sub>2</sub>/CdS electrode with carbon counter electrode (seen in Fig. 3b). Upon the CdS-sensitized TiO<sub>2</sub> electrodes by 6 screen printing cycles, comparison between Pt and carbon counter electrodes for QDSCs was performed. As shown in Fig. 3c, the CdS QDSCs with carbon electrode can present 3.1 mA cm<sup>-2</sup> of  $J_{sc}$ , 730 mV of  $V_{oc}$ , 60.0% of FF and 1.34% of  $\eta$ , while the device with Pt electrode only presents 2.2 mA cm<sup>-2</sup> of  $J_{sc}$ , 730 mV of  $V_{oc}$ , 57.6% of FF and 0.91% of  $\eta$ .

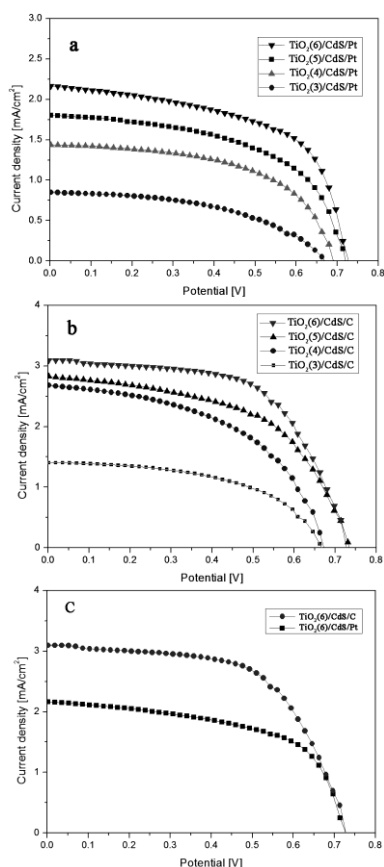


Fig. 3. The photocurrent-voltage ( $J$ - $V$ ) characteristics of TiO<sub>2</sub>( $n$ )/CdS electrodes with (a) Pt and (b) carbon counter electrode, and (c) TiO<sub>2</sub>(6)/CdS electrode Pt and carbon counter electrode.

Table 1 lists the photovoltaic parameters of the CdS QDSCs based on TiO<sub>2</sub> nanoporous electrodes with various screen printing cycles( $n$ ). The short-circuit current density ( $J_{sc}$ ) and power conversion efficiency( $\eta$ ) increased with  $n$ . The open-circuit voltage ( $V_{oc}$ ) is 0.67-0.73V and is almost independent of  $n$ . The best  $\eta$  is 1.34% for the TiO<sub>2</sub>(6)/CdS electrode with carbon counter electrode. The results indicate that the carbon counter electrode has a better performance than Pt counter electrode in these CdS QDSCs.

Table 1. Parameters obtained from the photocurrent-voltage ( $J$ - $V$ ) measurements of the QDSCs prepared with various electrodes.

Electrodes	$J_{sc}$ (mA/cm <sup>2</sup> )	$V_{oc}$ (V)	FF (%)	Efficiency (%)
TiO <sub>2</sub> (3)/CdS/Pt	0.8	0.67	48.1	0.27
TiO <sub>2</sub> (4)/CdS/Pt	1.4	0.69	55.4	0.55
TiO <sub>2</sub> (5)/CdS/Pt	1.8	0.72	54.4	0.70
TiO <sub>2</sub> (6)/CdS/Pt	2.2	0.73	57.6	0.91
TiO <sub>2</sub> (3)/CdS/C	1.4	0.67	52.5	0.49
TiO <sub>2</sub> (4)/CdS/C	2.7	0.67	50.0	0.90
TiO <sub>2</sub> (5)/CdS/C	2.8	0.73	54.0	1.12
TiO <sub>2</sub> (6)/CdS/C	3.1	0.73	60.0	1.34

#### 4. Conclusions

The CdS QDSCs based on screen printed TiO<sub>2</sub> nanoporous electrodes have been successfully prepared. TiO<sub>2</sub>/CdS electrode showed enhancement and broadening of absorption spectrum in visible light, in comparison with the plain TiO<sub>2</sub> electrode. The best conversion efficiency of the TiO<sub>2</sub>(6)/CdS electrode with carbon counter electrode showed 1.34%, which is higher than that of the TiO<sub>2</sub>(6)/CdS electrode with Pt counter electrode.

#### Acknowledgement

This work is supported by the National Basic Research Program of China (2009CB939704) and the Important Project of Ministry of Education of China (309021).

#### References

- [1] P. V. Kamat, *J. Phys. Chem. C* **112**(48), 18737 (2008).
- [2] D. R. Baker, P. V. Kamat, *Adv. Funct. Mater.* **19**(5), 805 (2009).
- [3] Y. J. Shen, Y. L. Lee, *Nanotechnology* **19**(4), 7 (2008).
- [4] H. J. Lee, J. H. Yum, H. C. Leventis, S. M. Zakeeruddin, S. A. Haque, P. Chen, S. I. Seok, M. Grätzel, M. K. Nazeeruddin, *J. Phys. Chem. C*

- 112**(30), 11600 (2008).
- [5] J. H. Bang, P. V. Kamat, *Adv. Funct. Mater.* **20**(12), 1970 (2010).
- [6] N. Zhao, T. P. Osedach, L. Y. Chang, S. M. Geyer, D. Wanger, M. T. Binda, A. C. Arango, M. G. Bawendi, V. Bulovic, *ACS Nano* **4**(7), 3743 (2010).
- [7] A. Tubtimtae, K. L. Wu, H. Y. Tung, M. W. Lee, G. J. Wang, *Electrochem. Commun.* **12**(9), 1158 (2010).
- [8] L. M. Peter, K. G. U. Wijayantha, D. J. Riley, J. P. Waggett, *J. Phys. Chem. B* **107**(33), 8378 (2003).
- [9] X. F. Gao, H. B. Li, W. T. Sun, Q. Chen, F. Q. Tang, L. M. Peng, *J. Phys. Chem. C* **113**(18), 7531 (2009).
- [10] P. Wang, S. Zakeeruddin, J. Moser, R. Humphry-Baker, P. Comte, V. Aranyos, A. Hagfeldt, M. Nazeeruddin, M. Grätzel, *Adv. Mater.* **16**(20), 1806 (2004).
- [11] R. Vogel, P. Hoyer, H. Weller, *J. Phys. Chem.* **98**(12), 3183 (1994).
- [12] M. T. Trinh, A. J. Houtepen, J. M. Schins, T. Hanrath, J. Piris, W. Knulst, A. P. L. M. Goossens, L. D. A. Siebbeles, *Nano Lett.* **8**(6), 1713 (2008).
- [13] C. H. Chang, Y. L. Lee, *Appl. Phys. Lett.* **91**(5), 3 (2007).
- [14] W. T. Sun, Y. Yu, H. Y. Pan, X. F. Gao, Q. Chen, L. M. Peng, *J. Am. Chem. Soc.* **130**(4), 1124 (2008).
- [15] Y. S. L. Yuh Lang Lee, *Adv. Funct. Mater.* **19**(4), 604 (2009).
- [16] J. M. Kroon, N. J. Bakker, H. J. P. Smit, P. Liska, K. R. Thampi, P. Wang, S. M. Zakeeruddin, M. Grätzel, A. Hinsch, S. Hore, U. Würfel, R. Sastrawan, J. R. Durrant, E. Palomares, H. Pettersson, T. Gruszecki, J. Walter, K. Skupien, G. E. Tulloch, *Prog. Photovoltaics Res. Appl.* **15**(1), 1 (2007).
- [17] K. Li, Y. Luo, Z. Yu, M. Deng, D. Li, Q. Meng, *Electrochem. Commun.* **11**(7), 1346 (2009).
- [18] W. J. Hong, Y. X. Xu, G. W. Lu, C. Li, G. Q. Shi, *Electrochem. Commun.* **10**(10), 1555 (2008).
- [19] T. Hino, Y. Ogawa, N. Kuramoto, *Carbon* **44**(5), 880 (2006).
- [20] K. Suzuki, M. Yamaguchi, M. Kumagai, S. Yanagida, *Chem. Lett.* **32**(1), 28 (2003).
- [21] K. X. Li, Z. X. Yu, Y. H. Luo, D. M. Li, Q. B. Meng, *J. Mater. Sci. Technol.* **23**, 577 (2007).
- [22] Z. Huang, X. H. Liu, K. X. Li, D. M. Li, Y. H. Luo, H. Li, W. B. Song, L. Q. Chen, Q. B. Meng, *Electrochem. Commun.* **9**(4), 596 (2007).
- [23] K. Imoto, K. Takahashi, T. Yamaguchi, T. Komura, J. Nakamura, K. Murata, *Sol. Energy Mater. Sol. Cells* **79**(4), 459 (2003).
- [24] T. N. Murakami, S. Ito, Q. Wang, M. K. Nazeeruddin, T. Bessho, I. Cesar, P. Liska, R. Humphry-Baker, P. Comte, P. Pechy, M. Grätzel, *J. Electrochem. Soc.* **153**(12), A2255 (2006).
- [25] M. Grätzel, *Nature* **414**(6861), 338 (2001).

---

\* Corresponding author: opluse@whut.edu.cn